

1. RESIDUAL MONTE CARLO TREATMENT OF THE TIME VARIABLE

Another area of potential improvement for the HOLO method is in the time discretization of the system. We have investigated using MC integration of the time derivative in the HO solver and introducing extra consistency terms into the LO equations. The goal is to produce a more accurate solution in optically thin regions where particles transport a long distance. A potential application is in stellar atmosphere calculations. In optically thin regions, the MC integration of the time-variable by IMC can produce greater accuracy, whereas an implicit Euler discretization will result in artificially fast propagation of energy. We hope to improve the efficiency of MC calculations in thin regions with the ECMC method while still preserving the accuracy of a MC treatment in the time variable. The time variable is included in the trial space for ECMC and the LO equations are closed consistently. We will not be performing adaptive refinement in time, so maintaining exponential convergence may not be possible. However, we still expect the residual MC formulation of the ECMC method to show improvement over standard MC.

1.1 Modifications to the HO equations

Inclusion of the time variable t in the trial space used by ECMC allows for no discretization of the transport operator \mathbf{L} . The transport operator, applied to the continuous intensity I becomes,

$$\mathbf{L}I(x, \mu, t) = \frac{1}{c} \frac{\partial I}{\partial t} + \sigma_t I + \mu \frac{\partial I}{\partial x} \quad (1.1)$$

The emission source is still treated with an implicit Euler discretization, which is similar to the approximation made in IMC. The ECMC algorithm is still specified the

same as in Sec. ??, however the residual source and MC tracking are now modified. Each batch is still estimating the error in the current estimate of $\tilde{I}(x, \mu, t)$, but now the time variable must be included in the inversion of the \mathbf{L} operator. The process of sampling and tracking in time step is detailed in literature[?, 1, ?, ?], but a brief outline is given in the remainder of this section, as well as the definition for the trial space and associated tallies.

1.1.1 The Doubly-Discontinuous Trial Space

It is necessary to define the time trial space so that we can explicitly define the residual for sampling. This trial space is similar to the LDD trial space used for the space variable in Sec. ??, however the solution is a constant value over the interior of the time step. This step, doubly-discontinuous trial space is defined as

$$\tilde{I}(x, \mu, t) = \begin{cases} \tilde{I}^n(x, \mu) & t = t^n \\ \bar{I}(x, \mu) & t \in (t^n, t^{n+1}) \\ & t = t^{n+1} \end{cases} \quad (1.2)$$

where we have used \bar{I} to denote the time-averaged value of the intensity over the interior of the time step and $\tilde{I}(x, \mu)$ is an LDFE projection in x and μ . An illustration of the time variable for this trial space is depicted in Fig. 1.1. There is a projection error in that we have used the LDFE space-angle projection to represent the intensity from the previous time step. However, with sufficient noise reduction and mesh resolution this should not be a large error as compared to IMC.

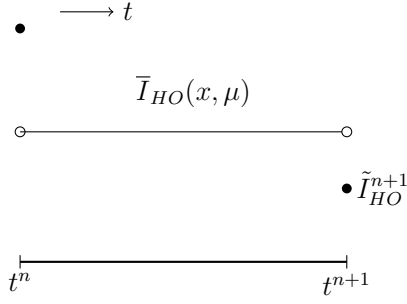


Figure 1.1: Step doubly-discontinuous representation of t for the HO solution.

The choice of this trial space will provide a projection for all the desired unknowns to exactly produce the moment equations, i.e., the time-averaged, end of time step, and previous time step values for the intensity. Temporally, these are the only unknowns that appear in equations that have been integrated over a time step to produce a balance statement. Another reason for this choice is that it allows for infrastructure for computing the residual from the time-discrete case. This trial space has one major drawback, in that some particles must reach the end of the time step, which can lead to poor statistics in optically thick problems. This is troubling, because in such problems you don't need much correction in the time variable. Alternatively, an LDFE representation could be used in the time variable. The linear representation would produce less noise because all particle tracks contribute to the slope, rather than just those that reach the end of the time step, although it would produce an approximate projection error for the end of time step intensity that is not produced with a discontinuity at the end of the time step. The linear representation in time would also produce a more accurate reconstruction of the scattering source in time. However, a linear representation requires the sampling algorithm to be significantly modified because the L_1 integral for computing the residual magnitude is

now significantly complicated by the tri-linear function. A possible way to sample this source is discussed in Appendix for completeness, but it has not been rigorously investigated.

1.1.2 Residual Source Definition and Sampling

The residual is defined as $r = q^{n+1} - \mathbf{L}\tilde{I}(x, \mu, t)$, where

$$q^{n+1} = (\sigma_a ac(T_{LO}^{n+1})^4(x) + \sigma_s \bar{\phi}) \quad (1.3)$$

is a constant in time. We have assumed a constant reconstruction for the scattering source in time. If the system is scattering dominated, this may be a poor approximation. Substitution of Eq. (1.2) for I produces a uniform source in time, as well as a δ -function source at the beginning and end of the time step, which is written as

$$r(x, \mu, t) = \bar{r}(x, \mu) + r^n(x, \mu)\delta^+(t - t^n) + r^{n+1}(x, \mu)\delta^-(t - t^{n+1}), \quad t \in [t^n, t^{n+1}] \quad (1.4)$$

We will look at each component individually. The first residual term is a constant in time with representation

$$\bar{r}(x, \mu) = q - \mu \frac{\partial \bar{I}(x, \mu)}{\partial x} - \sigma_t \bar{I}(x, \mu) \quad (1.5)$$

Evaluation of the above function produces both face and volumetric sources, similar to in the discrete case. To sample x and μ from the face and volume distributions, the same rejection procedure can be used as for Eq. (??) and detailed in [3]. The time variable can then be sampled uniformly over the time step, i.e., $t = t^n + \eta\Delta t$, where η is a uniform random variable with support $(0, 1)$.

The second source has definition

$$r^n(x, \mu) = -\frac{1}{c} \frac{\partial \bar{I}(x, \mu)}{\partial t} \Big|_{t=t^n} = -\frac{1}{c} \left(\bar{I}(x, \mu) - \tilde{I}^n(x, \mu) \right) \quad (1.6)$$

This source is a LDFE space and angle volumetric source. The rejection sampling procedure is used to sample x and μ . All particles sampled from this source begin tracking with $t = t^n$.

The final source term is

$$r^{n+1}(x, \mu) = -\frac{1}{c} \frac{\partial \bar{I}(x, \mu)}{\partial t} \Big|_{t=t^{n+1}} = -\frac{1}{c} \left(\tilde{I}^{n+1}(x, \mu) - \bar{I}(x, \mu) \right). \quad (1.7)$$

The source r^{n+1} can be treated using the same analytic treatment as the outflow face source in the LDD trial space, detailed in Sec. ??; the source at the end of the time step is never sampled because its contribution to I^{n+1} can be analytically computed. To treat the sources this way, the solution for $\tilde{I}^{n+1}(x, \mu)$ is initialized to the value of $\bar{I}(x, \mu)$ before a batch of particles begins. Then, error particles that reach the end of the time step, referred to as “census” particles, contribute a standard score to the projection $\tilde{I}^{n+1}(x, \mu)$.

With these definitions, it is thus only necessary to sample from the two sources. Using composite-rejection sampling [4]. A discrete probability distribution is sampled to determine which source is sampled. The algorithm is

1. Sample uniform random number η
2. If $\eta < \|r^n\|_1 / (\|r^n\|_1 + \|r^{n+1}\|_1)$:
 - Sample from r^n source using rejection sampling
 - Sample t uniformly over (t^n, t^{n+1}) .

3. Else:

- Sample from \bar{r} source

All L_1 integrals can be analytically integrated using the same numerics as in the time-discrete case. Using the systematic sampling algorithm, as described in Sec. ?? is performed similarly. However, the choice of source is only made locally over that space-angle element. In that case, the element is chosen systematically, then the choice of r^n or \bar{r} is made.

1.1.3 Importance Sampling on Interior of Time Step

As an attempt to reduce variance in the estimate of $\tilde{\epsilon}^{n+1}(x, \mu)$, we use important sampling in the time variable. Systematic sampling is still used for determining the cell of interest, and sampling as described above is used to determine which source is sampled, based on the appropriate probabilities described in the previous section. However, when the interior source $\bar{r}(x, \mu)$ is sampled, we use importance sampling for the conditional sampling of the uniform time step. The goal is to ensure that some histories reach the end of the time step. In order to do this, we sample from a modified PDF such that a fraction p_{end} of particles sampled from $\bar{r}(x, \mu)$ are born with $t \in (t^{end}, t^{n+1})$. We define $t^{end} = t^{n+1} - M/(c\sigma_t)$, where M is the desired number of MFP of travel the particle will undergo from the end of the time step (e.g., 2 or 3). The weights of particles sampled from this distribution must be modified to prevent source biasing.

The new PDF to be sampled from is

$$f^*(t) = \begin{cases} \frac{1 - p_{end}}{t^{end} - t^n} & 0 < t < t^{end} \\ \frac{p_{end}}{t^{n+1} - t^{end}} & t^{end} \leq t < t^{n+1} \\ 0 & \text{elsewhere} \end{cases} \quad (1.8)$$

The original PDF is $f(t) = 1/\Delta t$, for $t \in (t^n, t^{n+1})$. Thus, using the standard procedure for importance sampling[4], the starting time t_{start} is sampled from $f^*(t)$, and then weights are multiplied by the factor $f(t_{\text{start}})/f^*(t_{\text{start}})$. This procedure is not perfect in that if a particle is moving from an optically thin to an optically thick region, it is not guaranteed to reach census. However, this case does not introduce bias.

1.1.4 Tracking and Tallying in Time

Because our LO equations will be integrated over the time step, we only need to perform MC tracking for $t \in [t^n, t^{n+1}]$. The initial time for the particle is sampled as described in the previous section. In inverting the \mathbf{L} operator, particles are tracked until they reach the end of the time step. Path lengths are sampled or the weight is exponentially attenuated as before (e.g., Sec. ??). As a particle travels from position x_o to x_f , with direction μ , the time is updated as

$$t^f = t^0 + \frac{|x_f - x_o|}{c\mu} \quad (1.9)$$

where c is the speed of light. For analog path-length sampling, if $t^f > t^{n+1}$ then t^f is adjusted to t^{n+1} and the path length is adjusted accordingly. For continuous weight deposition, particles are only tracked until they reach t^{n+1} . A proof that this process of tracking particles is a MC solution to an integral equation that is exactly inverse to the \mathbf{L} operator is detailed in [?, ?].

Tallies must be adjusted to account for the averaging over the time step, and to compute the intensity at the end of time step. To produced the time-averaged representation $\bar{I}(x, \mu)$, requires estimators for the average, x , and μ moments of the

error, e.g.,

$$\bar{\epsilon}_{x,ij} = \frac{1}{\Delta t} \frac{6}{h_j} \int_{t^n}^{t^{n+1}} dt \int_{x_{i-1/2}}^{x_{i+1/2}} dx \int_{\mu_{j-1/2}}^{\mu_{j+1/2}} d\mu \left(\frac{x - x_j}{h_i} \right) \epsilon(x, \mu, t) \quad (1.10)$$

with a similar definition for the average and μ moments. In implementation, we have included the $\frac{1}{\Delta t}$ factor in the definition of the residual source, so the estimators are

$$\hat{\epsilon}_{x,ij} = \frac{1}{N_{hist}} \frac{6}{h_j} \sum_{n=1}^{N_{hist}} \frac{s_n}{h_i h_j} w_j (x_c - x_i) \quad (1.11)$$

where $\sum_{n=1}^N w_n = \|r(x, \mu, t)\|_1$, x_c is the center of the n -th path length, and s_n is the path length for the n -th path length in the $x - \mu$ cell.

Moments of $I^{n+1}(x, \mu)$ must be estimated to represent the end of time step intensity. For example, the moment of the error at the end of time step is

$$\epsilon_{x,ij}^{n+1} = \frac{6}{h_i} \iint_{\mathcal{D}_{ij}} \left(\frac{x - x_i}{h_i} \right) \epsilon(x, \mu, t^{n+1}) dx d\mu \quad (1.12)$$

The estimators for these moments are a generalization of the census tallies used in IMC [?, ?]. The tallies are based on the definition of the intensity as $I(x, \mu, t) = ch\nu N(x, \mu, t)$ given in Eq. (??), similar to collision estimators [4, ?]. Based on the definition of the residual, the estimator for the x moment is

$$\epsilon_{x,ij}^{n+1} = \frac{1}{N_{hist}} \frac{6}{h_j h_i} \sum_{n=1}^{N_{hist}} c w_j \Delta_t (x_c - x_i) \quad (1.13)$$

Similar tallies are defined for the other space-angle moments. These tallies can be exceptionally noisy because only particles that reach the end of the time step contribute.

REWRITE The factors of delta t actually have to do with the fact that when I

compute the L1 norm of the residual, I dont integrate over time. If i did, then this is all fine.

1.2 LO Closure

The LO equations must be modified to have a closure in time for consistency with the HO equations. The goal is to not add additional equations to solve for the time-dependent unknowns, rather than just using closure. Previous work has enforced consistency by subtract the continuous HO solution from a BE discretization of the discretized time-derivatives to add an artificial term [7]. This has the added benefit that the LO solver exclusively deals in time-averaged unknowns for radiation terms in the equations. We will alternatively use a parametric closure in the time variable, similar to the spatial closures discussed in the Sec. ???. The time-integrated equations will have primarily time-averaged values, which is desired. Additionally, the closure produces LO equations that have the same numerical difficulty to solve as the fully-discrete LO equations, but have the potential to preserve the accuracy of the MC integration in time, upon non-linear convergence of the system. A closure relation is used to eliminate the end of time step moments present from the time derivative term. We will investigate different parametric forms of the closure for robustness. Once the time-averaged unknowns have been calculated, the time closures can be used to advance to the end of time step values for the next time step.

1.2.1 Derivation of Time-Averaged Moment Equations

The time-continuous radiation equations are integrated in space and angle the same as before. For example, the L and $+$ moment equation is

$$\begin{aligned} \frac{1}{c} \frac{\partial}{\partial t} \langle \phi \rangle_L^+ - 2 \left(\mu_{i-1/2} I_{i-1/2} \right)^+ + \langle \mu I \rangle_{L,i}^+ + \langle \mu I \rangle_{R,i}^+ + \sigma_{t,i} h_i \langle \phi \rangle_{L,i}^+ - \frac{\sigma_{s,i} h_i}{2} \left(\langle \phi \rangle_{L,i}^+ + \langle \phi \rangle_{L,i}^- \right) \\ = \frac{h_i}{2} \langle \sigma_a a c T^4 \rangle_{L,i} \quad (1.14) \end{aligned}$$

This equation is then integrated over the time step, and the emission source is assumed implicit. The same manipulations can be performed on the streaming term to form angular consistency terms, but the weighting fluxes are now time-averaged values. Thus, the angular consistency terms are computed with $\bar{I}(x, \mu)$. The equations with time-averaged consistency terms are

$$\begin{aligned} \frac{\langle \phi \rangle_{L,i}^{+,n+1} - \langle \phi \rangle_{L,i}^{+,n}}{c\Delta t} - 2\bar{\mu}_{i-1/2}^+ \bar{\phi}_{i-1/2}^+ + \{\bar{\mu}\}_{L,i}^+ \langle \bar{\phi} \rangle_{L,i}^+ + \{\bar{\mu}\}_{R,i}^+ \langle \bar{\phi} \rangle_{R,i}^+ + \sigma_{t,i}^{n+1} h_i \langle \bar{\phi} \rangle_{L,i}^{n+1,+} \\ - \frac{\sigma_{s,i} h_i}{2} (\langle \bar{\phi} \rangle_{L,i}^+ + \langle \bar{\phi} \rangle_{L,i}^-) = \frac{h_i}{2} \langle \sigma_a^{n+1} ac T^{n+1,4} \rangle_{L,i}, \quad (1.15) \end{aligned}$$

These equations are exact at this point.

1.2.2 Closure

The closure relations in time are different than the closure relations for the spatial variable because we do not have a time slope. The following closure is a modified diamond relation:

$$I^{n+1} = 2\gamma \bar{I} - I^n \quad (1.16)$$

where γ is the closure factor and \bar{I} is the time-averaged intensity. A modified implicit discretization can also be used

$$I^{n+1} = \gamma \bar{I} \quad (1.17)$$

A closure relation must be used to eliminate the unknowns at t^{n+1} from each of the equations, with the values from the previous time step taken as a known quantity. Thus, it is necessary to have a closure relation for each moment and half range, producing four closure parameters per spatial cell. The closure relations for

the L moment and the modified diamond relation are

$$\langle \phi \rangle_{L,i}^{\pm,n+1} = 2\gamma_{L,i}^{\pm} \langle \bar{\phi} \rangle_{L,i}^{\pm} - \langle \phi \rangle_{L,i}^{\pm,n} \quad (1.18)$$

with equivalent definitions for the R moment. Substitution of the above equation into Eq. (??)

$$\begin{aligned} \frac{2}{c\Delta t} [\gamma_{L,i}^+ \langle \phi \rangle_L^{+,n+1} - \langle \phi \rangle_L^{+,n}] - 2\bar{\mu}_{i-1/2}^+ \bar{\phi}_{i-1/2}^+ + \{\mu\}_{L,i}^{n+1,+} \langle \phi \rangle_{L,i}^{n+1,+} + \{\mu\}_{R,i}^{n+1,+} \langle \phi \rangle_{R,i}^{n+1,+} + \left(\sigma_{t,i}^{n+1} + \frac{1}{c\Delta t} \right) h \\ - \frac{\sigma_{s,i} h_i}{2} (\langle \phi \rangle_{L,i}^{n+1,+} + \langle \phi \rangle_{L,i}^{n+1,-}) = \frac{h_i}{2} \langle \sigma_a^{n+1} a c I^{n+1,4} \rangle_{L,i} + \frac{h_i}{c\Delta t} \langle \phi \rangle_{L,i}^{n,+}, \quad (1.19) \end{aligned}$$

The value of $\gamma_{L,i}^+$, $\gamma_{R,i}^+$, $\gamma_{L,i}^-$, and $\gamma_{R,i}^-$ are computed with the trial-space representation of $I^{HO}(x, \mu, t)$ substituted into Eq. (1.16) and Eq. (1.17). One potential benefit of the time closure parameters is that \bar{I}^{HO} will be most different from $I^{HO,n+1}$ in problems that are optically thin. In such problems, σ_a is small, leading to an optically thin problem. However, there may be difficulties in the MPV problems where the problems are tightly coupled and nonlinear, but can lead to a large change over a time step.

REFERENCES

- [1] J. A. Fleck, Jr. and J. D. Cummings, Jr. An implicit monte carlo scheme for calculating time and frequency dependent nonlinear radiation transport. *J. Comput. Phys.*, 8(3):313–342, December 1971.
- [2] Elmer Eugene Lewis and Warren F Miller. *Computational methods of neutron transport*. John Wiley and Sons, Inc., New York, NY, 1984.
- [3] J.R. Peterson. Exponentially Convergent Monte Carlo for the 1-d Transport Equation. Master’s thesis, Texas A&M, 2014.
- [4] J.K. Shultis and W.L. Dunn. *Exploring Monte Carlo Methods*. Academic Press, Burlington, MA 01803, 2012.
- [5] ”Weston M. Stacey”. *”Nuclear Reactor Physics”*. Wiley, 2007.
- [6] T.A. Wareing. *Asymptotic diffusion accelerated discontinuous finite element methods for transport problems*. PhD thesis, Michigan, 1991.
- [7] Allan B. Wollaber, H. Park, R.B. Lowrie, R.M. Rauenzahn, and M.E. Cleveland. Radiation hydrodynamics with a high-order, low-order method. In *ANS Topical Meeting, International Topical Meeting on Mathematics and Computation*, Nashville Tennessee, 2015.

APPENDIX A

DERIVATIONS AND EQUATIONS FOR THE LO SYSTEM

A.1 Useful Moment Relations for LO Equations

There are several relations between various moment definitions that are useful in derivation and manipulation of the LO equations. The following are derived for $\phi(x)$, but can be applied to general moments of functions. The volumetric average terms can be eliminated in terms of the L and R moments from the relation $b_{L,i}(x) + b_{R,i}(x) = 1$.

$$\phi_i = \frac{1}{h_i} \int_{x_{i-1/2}}^{x_{i+1/2}} \phi(x) dx \quad (\text{A.1})$$

$$= \frac{1}{h_i} \left(\int_{x_{i-1/2}}^{x_{i+1/2}} b_{L,i}(x) \phi(x) dx + \int_{x_{i-1/2}}^{x_{i+1/2}} b_{R,i}(x) \phi(x) dx \right) \quad (\text{A.2})$$

$$= \frac{1}{2} (\langle \phi \rangle_{L,i} + \langle \phi \rangle_{R,i}) \quad (\text{A.3})$$

A similar relation can be derived for the first moment in space as

$$\phi_{x,i} = \frac{3}{2} (\langle \phi \rangle_{R,i} - \langle \phi \rangle_{L,i}) \quad (\text{A.4})$$

The above relations can be inverted to derived a relation for the L and R moments in terms of the slope and average moments. These moment expressions are defined purely in terms of integrals, and are independent of the chosen spatial representation

Once a linear relation on the interior has been assumed, there are other useful closures that can be derived. The standard linear interpolatory expansion, for the

positive half-range, is restated here:

$$\phi^+(x) = \phi_{L,i}^+ b_{L,i}(x) + \phi_{R,i}^+ b_{R,i}(x) \quad (\text{A.5})$$

Using this expansion, one can derive a relation between the outflow from a cell and the hat function moments that is equivalent to the standard LDFE Galerkin method:

$$\phi_{i,R}^+ = 2\langle\phi\rangle_{R,i}^+ - \langle\phi\rangle_{L,i}^+ \quad (\text{A.6})$$

this linear relation also defines the value for $\phi_{i,L}^+$.

To eliminate the LO unknowns in a manner that is equivalent to lumping the discrete system, the following expression can be used for the outflow from a cell

$$\phi_{i+1/2}^+ = \phi_i^+ + \frac{\phi_x^+}{3}, \quad (\text{A.7})$$

which in terms of the hat function moments is equivalent to $\phi_{i+1/2}^+ = \langle\phi\rangle_{R,i}^+$. Inserting this expression into Eq. (??), and using the same definition for the linear representation over the interior of $\phi_{i+1/2}^+(x) = \phi_{L,i}^+ b_{L,i}(x) + \phi_{R,i}^+ b_{R,i}(x)$, will produce an equivalent set of unknowns as a linear discontinuous method with a lumped representation for the radiation. The temperature equation must be independently lumped. This relation preserves the average within a cell but modifies the first moment.

A similar expression produces a lumped-equivalent representation on the interior of the cell:

$$\phi_{i,R}^+ = \phi_i^+ + \frac{\phi_x^+}{3}, \quad (\text{A.8})$$

The moment equations are not modified by using this expression, however the interpretation of the moments as a linear representation over the cell has been altered.

This allows for us to ensure a lumped representation on the interior while still using the HO solution to eliminate the outflow from the equations.

A.2 Newtons Method for the LO Equations

Because we have only considered problems with constant densities and heat capacities, the linearization described below is in terms of temperature T rather than material internal energy, for simplicity. However, the linearization can be formed in terms of internal energy to apply this method to a general equation of state.

To formulate the Newton iterations, the Planckian source is linearized in the material and radiation equations (Eq. (??) & Eq. (??)). Application of the first order Taylor expansion in time to the implicit emission source $B(T^{n+1})$, about some temperature T^* at some time $t^* \in [t^n, t^{n+1}]$, yields

$$\sigma_a^{n+1} acT^{4,n+1} \simeq \sigma_a^* ac [T^{*4} + (T^{n+1} - T^*)4T^{*3}] \quad (\text{A.9})$$

where $\sigma_a^* \equiv \sigma_a(T^*)$. Substitution of this expression into Eq. (??) yields

$$\rho c_v \left(\frac{T^{n+1} - T^n}{\Delta t} \right) = \sigma_a^* \phi^{n+1} - \sigma_a^* ac [T^{*4} + (T^{n+1} - T^*)4T^{*3}]. \quad (\text{A.10})$$

Algebraic manipulation of this equation yields an expression for $T^{n+1} - T^*$:

$$(T^{n+1} - T^*) = \frac{\frac{\sigma_a^* \Delta t}{\rho c_v} [\phi^{n+1} - acT^{*4}] + (T^n - T^*)}{1 + \sigma_a^* ac \Delta t \frac{4T^{*3}}{\rho c_v}}.$$

This expression is substituted back into Eq. (A.9) to form an explicit approximation for the emission source at t^{n+1} as

$$\sigma_a acT^{4,n+1} \simeq \sigma_a^* (1 - f^*) \phi^{n+1} + f^* \sigma_a^* acT^{4,n} + \rho c_v \frac{1 - f^*}{\Delta t} (T^n - T^*) \quad (\text{A.11})$$

where $f^* = [1 + \sigma_a^* c \Delta t 4a T^{*3} / (\rho c_v)]^{-1}$ is often referred to as the Fleck factor [1].

Next, the above equation must be spatially discretized. Application of the L spatial moment yields

$$\begin{aligned} \langle \sigma_a^* a c T^{4,n+1} \rangle_{L,i} &= \sigma_{ai}^* (1 - f_i^*) \langle \phi^{n+1} \rangle_{L,i} + f_i^* \sigma_{ai}^* a c \left(\frac{2}{3} T_{L,i}^{4,n} + \frac{1}{3} T_{R,i}^{4,n} \right) \\ &\quad \rho_i c_{vi} \frac{1 - f_i^*}{\Delta t} \left[\frac{2}{3} (T_{L,i}^n - T_{L,i}^*) + \frac{1}{3} (T_{R,i}^n - T_{R,i}^*) \right], \quad (\text{A.12}) \end{aligned}$$

where $T^{4,n}$ and T^n have been assumed LD and f^* is assumed constant over a cell, i.e., $f_i^* \equiv \sigma_a(T_i^*)$. The error introduced by a constant f^* approaches zero as the non-linearity is converged because T^* approaches T^{n+1} . Based on an estimate for T^* , Eq. (A.12) is an expression for the Planckian emission source in the radiation moment equations with an additional effective scattering source. A similar expression can be derived for $\langle \sigma_{a,i} a c T^4 \rangle_R$ and the right moment equations. The expressions for the emissions source is substituted into the radiation moment equations (Eq. (??)–(??)) to produce a linear system of equations for the new radiation intensity moments.

Once the linear equations have been solved for new radiation moments, new temperature unknowns can be estimated. To conserve energy, the same linearization and discretizations used to solve the radiation equation must be used in the material energy equation. Substitution of Eq. (A.12) into the material energy L moment equation ultimately yields

$$\begin{aligned} \frac{2}{3} T_{L,i}^{n+1} + \frac{1}{3} T_{R,i}^{n+1} &= \frac{f_i^* \sigma_{ai}^* \Delta t}{\rho c_v} \left[\langle \phi^{n+1} \rangle_{L,i} - a c \left(\frac{2}{3} T_{L,i}^{4,n} + \frac{1}{3} T_{R,i}^{4,n} \right) \right] + \\ &\quad (1 - f_i^*) \left(\frac{2}{3} T_{L,i}^* + \frac{1}{3} T_{R,i}^* \right) + f \left(\frac{2}{3} T_{L,i}^n + \frac{1}{3} T_{R,i}^n \right) \quad (\text{A.13}) \end{aligned}$$

A similar expression is produced for the R moment equation. This produces a local

matrix equation to solve for new T unknowns. If both the radiation and temperature unknowns are lumped, this matrix becomes diagonalized.

Based on these equations, the algorithm for solving the LO equations, with iteration index l , is defined as

1. Initialize T unknowns using T^n or the last estimate of T^{n+1} from previous LO solve
2. Build the LO system based on the effective scattering $(1 - f^l)$ and emission terms evaluated using T^l .
3. Solve the linearized LO system to produce an estimate for $\phi^{n+1,l}$.
4. Evaluate a new estimate of T^{n+1} unknowns using Eq. (A.13).
5. $T^* \leftarrow \tilde{T}^{n+1}$.
6. Repeat 2-5 until $(T^{n+1,k})^4$ and $\phi^{n+1,k}$ are converged.



Figure A.1: TAMU figure

A.3 Derivation of the WLA-DSA Equations

In this section, we derive the discretized diffusion equation and LD mapping equations that are used in the WLA-DSA equations. To simplify notation, we derive the equations from a generic transport equation (rather than the error equations) with isotropic scattering and source q_0 , i.e.,

$$\mu \frac{\partial I}{\partial x} + \sigma_t I = \frac{\sigma_s}{2} (\phi(x) + q_0). \quad (\text{A.14})$$

A.3.1 Forming a Continuous Diffusion Equation

First, a continuous spatial discretization of a diffusion equation is derived. The mean intensity ϕ will ultimately be assumed continuous at faces to produce a standard three-point finite-difference diffusion discretization. The zeroth and first μ moment of Eq. (A.14) produce the P_1 equations [2, 6], i.e.,

$$\frac{\partial J}{\partial x} + \sigma_a \phi = q_0 \quad (\text{A.15})$$

$$\sigma_t J + \frac{1}{3} \frac{\partial \phi}{\partial x} = 0. \quad (\text{A.16})$$

The spatial finite element moments (defined by Eq. (??) and (??)) are taken of the above equations. The mean intensity is assumed linear on the interior of the cell, i.e., $\phi(x) = \phi_L b_L(x) + \phi_R b_R(x)$, for $x \in (x_{i-1/2}, x_{i+1/2})$. Taking the left moment, evaluating integrals, and rearranging yields

$$J_i - J_{i-1/2} + \frac{\sigma_{a,i} h_i}{2} \left(\frac{2}{3} \phi_{L,i} + \frac{1}{3} \phi_{R,i} \right) = \frac{h_i}{2} \langle q \rangle_{L,i}, \quad (\text{A.17})$$

where J_i is the average of the flux J over the cell. The moments of q are not simplified to be compatible with the error equations which are in terms of moments. For the R moment

$$J_{i+1/2} - J_i + \frac{\sigma_{a,i} h_i}{2} \left(\frac{2}{3} \phi_{L,i} + \frac{1}{3} \phi_{R,i} \right) = \frac{h_i}{2} \langle q \rangle_{R,i}. \quad (\text{A.18})$$

The equation for the L moment is evaluated for cell $i+1$ and added to the R moment equation evaluated at i . The flux J is assumed continuous at $i+1/2$ to eliminate the face fluxes from the equations. The sum of the two equations becomes

$$J_{i+1} - J_i + \frac{\sigma_{a,i+1} h_{i+1}}{2} \left(\frac{2}{3} \phi_{L,i+1} + \frac{1}{3} \phi_{R,i+1} \right) + \frac{\sigma_{a,i} h_i}{2} \left(\frac{1}{3} \phi_{L,i} + \frac{2}{3} \phi_{R,i} \right) =$$

$$\frac{h}{2} (\langle q \rangle_{L,i+1} + \langle q \rangle_{R,i}) . \quad (\text{A.19})$$

The mean intensity is approximated as continuous at each face, i.e., $\phi_{L,i+1} = \phi_{R,i} \equiv \phi_{i+1/2}$. Adding the L and R moments of Eq. (A.16) together, with the continuous approximation for $\phi_{i+1/2}$, produces a discrete Fick's law equation [5]

$$J_i = -D_i \frac{\phi_{i+1/2} - \phi_{i-1/2}}{h_i}, \quad (\text{A.20})$$

where $D_i = 1/(3\sigma_{t,i})$. Substitution of Eq. (A.20) into Eq. (A.19) and rearranging yields the following discrete diffusion equation:

$$\begin{aligned} \left(\frac{\sigma_{a,i+1} h_{i+1}}{6} - \frac{D_{i+1}}{h_{i+1}} \right) \phi_{i+3/2} + \left(\frac{D_{i+1}}{h_{i+1}} + \frac{D_i}{h_i} + \frac{\sigma_{a,i+1} h_{i+1}}{3} + \frac{\sigma_{a,i} h_i}{3} \right) \phi_{i+1/2} \\ + \left(\frac{\sigma_{a,i} h_i}{6} - \frac{D_i}{h_i} \right) \phi_{i-1/2} = \frac{h_{i+1}}{2} \langle q \rangle_{L,i+1} + \frac{h_i}{2} \langle q \rangle_{R,i} . \end{aligned} \quad (\text{A.21})$$

To allow for the use of lumped or standard LD in these equations, we introduce the factor θ , with $\theta = 1/3$ for standard LD, and $\theta = 1$ for lumped LD. The diffusion equation becomes

$$\begin{aligned} \left(\frac{\sigma_{a,i+1} h_{i+1}}{4} (1 - \theta) - \frac{D_{i+1}}{h_{i+1}} \right) \phi_{i+3/2} + \left(\frac{D_{i+1}}{h_{i+1}} + \frac{D_i}{h_i} + \left(\frac{1 + \theta}{2} \right) \left[\frac{\sigma_{a,i+1} h_{i+1}}{2} + \frac{\sigma_{a,i} h_i}{2} \right] \right) \phi_{i+1/2} \\ + \left(\frac{\sigma_{a,i} h_i}{4} (1 - \theta) - \frac{D_i}{h_i} \right) \phi_{i-1/2} = \frac{h_{i+1}}{2} \langle q \rangle_{L,i+1} + \frac{h_i}{2} \langle q \rangle_{R,i} . \end{aligned} \quad (\text{A.22})$$

Summation over all cells forms a system of equations for ϕ at each face.

A.3.1.1 Diffusion Boundary Conditions

The upwinding in the LO system exactly satisfies the inflow boundary conditions, therefore a vacuum boundary condition is applied to the diffusion error equations.

The equation for the left moment at the first cell is given by

$$J_1 - J_{1/2} + \frac{\sigma_{a,i} h_i}{2} \left(\frac{1+\theta}{2} \phi_{L,i} + \frac{1-\theta}{2} \phi_{R,i} \right) = \frac{h_i}{2} \langle q \rangle_{L,i} , \quad (\text{A.23})$$

The Marshak boundary condition for the vacuum inflow at face $x_{1/2}$ is given as

$$J_{1/2}^+ = 0 = \frac{\phi_{1/2}}{4} + \frac{J_{1/2}}{2}, \quad (\text{A.24})$$

which can be solved for $J_{1/2}$. Substitution of the above equation and Eq. (A.20) into Eq. (A.23) gives

$$\left(\frac{1}{2} + \sigma_{a,1} h_1 \frac{1+\theta}{4} - \frac{D_1}{h_1} \right) \phi_{1/2} + \left(\sigma_{a,1} h_1 \frac{1-\theta}{4} - \frac{D_1}{h_1} \right) \phi_{3/2} = \frac{h_i}{2} \langle q \rangle_{L,1} \quad (\text{A.25})$$

A similar expression can be derived for the right-most cell.

A.3.2 Mapping Solution onto LD Unknowns

Solution of the continuous diffusion equation will provide an approximation to ϕ on faces, denoted as $\phi_{i+1/2}^C$. We now need to map the face solution onto the LD representation of ϕ . To do this, first we take the L and R finite element moments of the P_1 equations. A LDFE dependence is assumed on the interior of the cell for J and ϕ . Taking moments of Eq. (A.15) and simplifying yields

$$J_{i+1/2} - \frac{J_{L,i} + J_{R,i}}{2} + \frac{\sigma_{a,i} h_i}{2} \left(\frac{1}{3} \phi_{L,i} + \frac{2}{3} \phi_{R,i} \right) = \frac{h_i}{2} \langle q \rangle_{R,i} \quad (\text{A.26})$$

$$\frac{J_{L,i} + J_{R,i}}{2} - J_{i-1/2} + \frac{\sigma_{a,i} h_i}{2} \left(\frac{2}{3} \phi_{L,i} + \frac{1}{3} \phi_{R,i} \right) = \frac{h_i}{2} \langle q \rangle_{L,i} \quad (\text{A.27})$$

The moment equations for Eq. (A.16) are

$$\frac{1}{3} \left(\phi_{i+1/2} - \frac{\phi_{i,L} + \phi_{i,R}}{2} \right) + \frac{\sigma_{t,i} h_i}{2} \left(\frac{1}{3} J_{L,i} + \frac{2}{3} J_{R,i} \right) = 0 \quad (\text{A.28})$$

$$\frac{1}{3} \left(\frac{\phi_{i,L} + \phi_{i,R}}{2} - \phi_{i-1/2} \right) + \frac{\sigma_{t,i} h_i}{2} \left(\frac{2}{3} J_{L,i} + \frac{1}{3} J_{R,i} \right) = 0 \quad (\text{A.29})$$

The face terms $J_{i\pm 1/2}$ and $\phi_{i\pm 1/2}$ need to be eliminated from the system. First, the scalar intensity is assumed to be the value provided by the continuous diffusion solution at each face, i.e., $\phi_{i\pm 1/2} = \phi_{i\pm 1/2}^C$. Then, the fluxes are decomposed into half-range values to decouple the equations between cells. At $x_{i+1/2}$, the flux is composed as $J_{i+1/2} = J_{i+1/2}^+ + J_{i+1/2}^-$, noting that in this notation the half-range fluxes are $J_{i+1/2}^\pm = \pm \int_0^\pm \mu I(x_{i+1/2}, \mu) d\mu$ ¹. We approximate the incoming fluxes, e.g., $J_{i+1/2}^-$, based on $\phi_{i+1/2}^C$ and a P₁ approximation. The P₁ approximation provides the following relation [6]

$$\phi = 2(J^+ - J^-). \quad (\text{A.30})$$

At $x_{i+1/2}$, the above expression is solved for the incoming current $J_{i+1/2}^-$. The total current becomes

$$J_{i+1/2} = J_{i+1/2}^+ - J_{i+1/2}^- = 2J_{i+1/2}^+ - \frac{\phi_{i+1/2}^C}{2}, \quad (\text{A.31})$$

In the positive direction, at the right face, the values of ϕ and J are based on the LD representation within the cell at that face, i.e., $\phi_{R,i}$ and $J_{R,i}$. The standard P₁ approximation for the half-range fluxes is used[5], i.e.,

$$J^\pm = \frac{\gamma\phi}{2} \pm \frac{J}{2}, \quad (\text{A.32})$$

¹Typically, the half-range fluxes are defined with integrals weighted with $|\mu|$, but this notation would not be consistent with our definition of the half-range consistency terms

where γ accounts for the difference between the LO parameters and the true P_1 approximation. Thus, for the right face and positive half-range,

$$J_{i+1/2}^+ = \frac{\gamma}{2}\phi_{i,R} + \frac{J_{i,R}}{2} \quad (\text{A.33})$$

A similar expression can be derived for $x_{i-1/2}$. The total fluxes at each face are thus

$$J_{i+1/2} = \gamma\phi_{i,R} + J_{i,R} - \frac{\phi_{i+1/2}^C}{2} \quad (\text{A.34})$$

$$J_{i-1/2} = \frac{\phi_{i-1/2}^C}{2} - \gamma\phi_{i,L} + J_{i,L} \quad (\text{A.35})$$

Substitution of these results back into the LD balance equations and introduction of the lumping notation yields the final equations

$$\left(\gamma\phi_{i,R} + J_{i,R} - \frac{\phi_{i+1/2}^C}{2} \right) - \frac{J_{L,i} + J_{R,i}}{2} + \frac{\sigma_{a,i}h_i}{2} \left(\frac{(1-\theta)}{2}\phi_{L,i} + \frac{(1+\theta)}{2}\phi_{R,i} \right) = \frac{h_i}{2}\langle q \rangle_{R,i} \quad (\text{A.36})$$

$$\frac{J_{L,i} + J_{R,i}}{2} - \left(\frac{\phi_{i-1/2}^C}{2} - \gamma\phi_{i,L} + J_{i,L} \right) + \frac{\sigma_{a,i}h_i}{2} \left(\frac{(1+\theta)}{2}\phi_{L,i} + \frac{(1-\theta)}{2}\phi_{R,i} \right) = \frac{h_i}{2}\langle q \rangle_{L,i} \quad (\text{A.37})$$

$$\frac{1}{3} \left(\phi_{i+1/2}^C - \frac{\phi_{i,L} + \phi_{i,R}}{2} \right) + \frac{\sigma_{t,i}h_i}{2} \left(\frac{(1-\theta)}{2}J_{L,i} + \frac{(1+\theta)}{2}J_{R,i} \right) = 0 \quad (\text{A.38})$$

$$\frac{1}{3} \left(\frac{\phi_{i,L} + \phi_{i,R}}{2} - \phi_{i-1/2}^C \right) + \frac{\sigma_{t,i}h_i}{2} \left(\frac{(1+\theta)}{2}J_{L,i} + \frac{(1-\theta)}{2}J_{R,i} \right) = 0. \quad (\text{A.39})$$

The above equations are completely local to each cell and fully defined, including for boundary cells. For simplicity, we just take $\gamma = 1/2$. The system can be solved for the desired unknowns $\phi_{i,L}$, $\phi_{i,R}$, $J_{i,L}$, and $J_{i,R}$, which represent the mapping of $\phi_{i+1/2}^C$

onto the LD representation for $\phi^\pm(x)$.

APPENDIX B

SECOND APPENDIX WITH A LONGER TITLE - MUCH LONGER IN FACT

Text for the Appendix follows.



Figure B.1: TAMU figure

B.1 Appendix Section